DOI 10.31489/2023PH4/65-75

UDC 539.3

V.N. Ukrainets, S.R. Girnis, K.T. Makashev, V.T. Stanevich

Toraighyrov University, Pavlodar, Kazakhstan
(E–mail: vitnikukr@mail.ru, girnis@mail.ru, makashevkuanysh10@gmail.com, svt_18@mail.ru
**Corresponding authors e-mail: vitnikukr@mail.ru*

Dynamic response of unsupported and supported cavities in an elastic half-space under moving normal and torsional loads

This study explores the impact of uniformly moving normal and torsional loads along an infinitely long circular cylindrical cavity, situated within a half-space (body), on the behavior of the elastic half-space. The cavity is either unreinforced or reinforced by a thin-walled elastic shell. To describe the motion of the body and the shell, dynamic equations of elasticity theory in the Lamé potentials and equations of the classical shell theory are used, respectively. The equations are represented in coordinate systems moving together with the loads (cylindrical or Cartesian). The method of integral Fourier transform is used to determine the stress-strain state (SSS) of the half-space. The solution to this problem considers waves reflected from the boundary of the half-space, which occur during the movement of loads, instead of assuming the body is an elastic space like similar works. The results of numerical experiments are presented, illustrating the influence of the shell on the deformed state of the half-space boundary under the action of axisymmetric normal and shear loads, which are uniformly applied within a certain range and move at a constant speed.

Keywords: elastic half-space, body, cavity, cylindrical shell, moving load, velocity, displacement, stress.

Introduction

Lately, there has been a noticeable increase in studying the dynamic behavior of various engineering and structural systems due to the diverse types of moving loads they encounter. Such problems arise in the calculation of aerodromes under the influence of moving aircraft, tunnels, and underground pipelines under the influence of transport loads (loads that occur during the movement of intratunnel transport and the transportation of solid materials, liquids, and gases through pipelines) and so on. The rapid progress in modern technology, computational mathematics, and computer technologies has played a crucial role in stimulating this growing interest.

In the context of the tunnel and underground main pipeline dynamics subjected to transportation loads, the research typically focuses on model problems addressing the effect of a load on a cylindrical shell (the surface of the cavity if the tunnel is unsupported) situated within an elastic body. The load uniformly moves along the inner surface of the shell along its generatrix. In the case of deep placement of these structures, the body represents an elastic space, while in the case of shallow placement, it is an elastic half-space. Model problems of the tunnel and deep-buried transportation pipeline dynamics under the influence of transportation loads have been examined in numerous scientific studies. The number of publications dedicated to this issue is relatively small in the case of shallow placement of these structures due to the more complex nature of the problem formulation. Recent years have seen a notable increase in published works that deserve recognition [1–6]. In these studies, numerical investigations of the SSS of the body were conducted for the case when a normal moving load of various types acts on the cylindrical shell or the cavity surface. In articles [7, 8] similar investigations were conducted for the case of a normal axisymmetric load [7] and an axisymmetric torsional load [8] acting on an extremely long thin-walled circular cylindrical shell positioned in an elastic space. To describe the motion of both the body and the shell, the dynamic equations of elasticity theory and the equations of the classical theory of shells were used, represented in the moving cylindrical coordinate system. In [7], when the speed of the load's movement was subsonic, the Fourier transformation was applied to the moving axial coordinate for solving the problem. Dynamic equations of the theory of elasticity and classical shell theory equations were used to describe the motion of the body and shell, respectively. These equations were presented in a moving cylindrical coordinate system. In article [7], Fourier transformation was used to solve the problem, while in article [8], Fourier or Laplace transformation was applied with respect to the moving coordinate.

The present article provides a solution to the problem of the combined action of moving normal and torsional loads on an infinitely long thin-walled circular cylindrical shell or cavity surface in an elastic inertial half-space. Such action occurs during the rotational movement of cleaning devices in an underground pipeline [9], and it can also arise due to the inequality of dynamic loads transmitted to each of the rails laid in a cylindrical tunnel [10], whether supported by a shell or unsupported. In contrast to [7, 8] and similar works, the moving loads in this article can have an arbitrary form. Additionally, when solving the problem, the influence of waves reflected from the boundary of the half-space, which arise during the movement of loads, is taken into account.

Methods

The study is based on assumptions and equations of elasticity theory. To solve the problem, the method of integral Fourier transform is used. This allows us to consider moving loads distributed along the shell's axis according to an arbitrary law and obtain the final expression of the solution without the need for summation.

Problem formulation and solution

Let's consider a homogeneous and isotropic body in Cartesian x, y, z and cylindrical r, θ, z coordinate systems, which have a common origin occupying a fixed position in space. The body is a linear elastic half-space ($x = h$), with its boundary free from loads and parallel to the z-axis. The body contains an elongated circular cylindrical cavity with a radius of R, the axis of which coincides with the x-axis (Fig. 1). The surface of the cavity can be rigidly connected to a thin shell with a thickness of h_0. Since the shell has a small thickness, we will assume that it contacts the body along its middle surface (Fig. 2). We will use the following notation for the physicomechanical properties of the body and shell materials. Poisson's ratio: ν (for the body), ν_0 (for the shell); shear modulus: μ (for the body), μ_0 (for the shell); density: ρ (for the body), ρ_0 (for the shell).

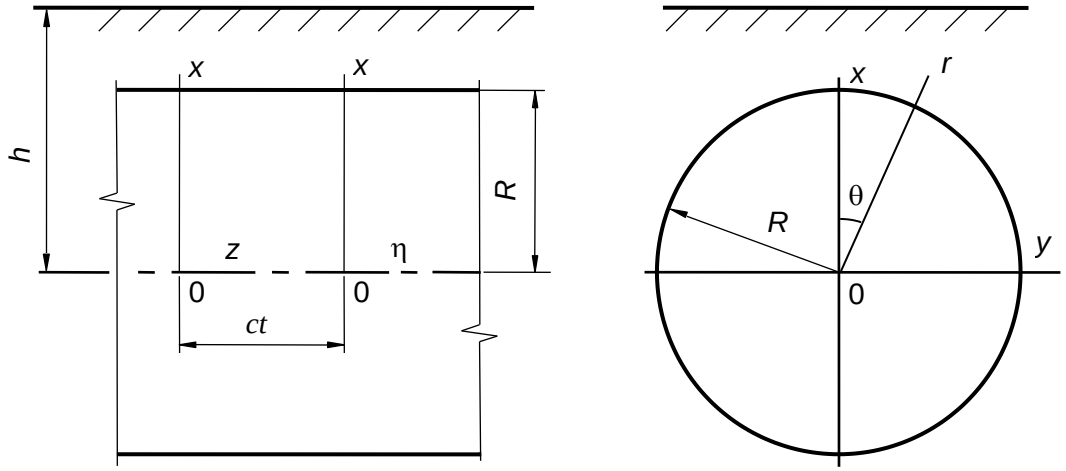

Figure 1. Half-space containing a circular cavity

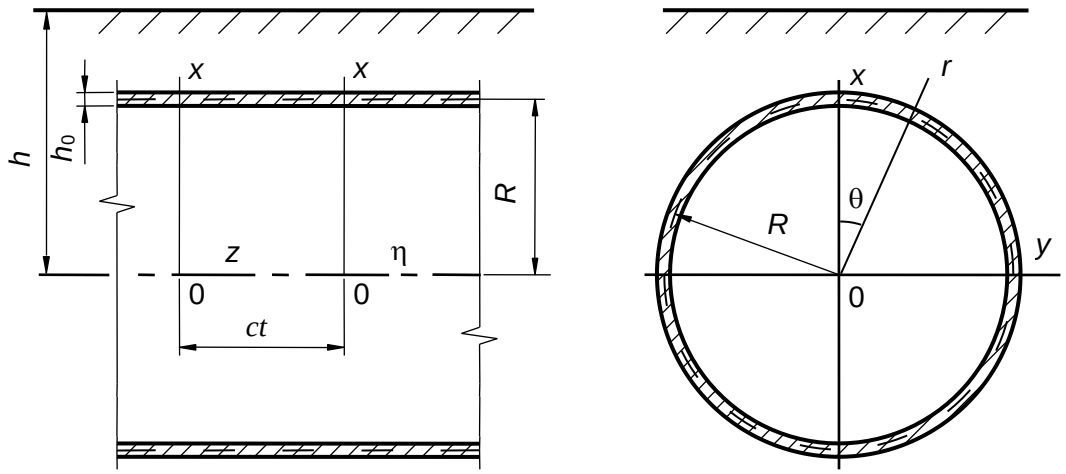

Figure 2. Half-space containing a circular shell

Figures illustrate normal and tangential (torsional) loads moving along the *z*-axis at a constant speed *c*, either on the surface of the cavity (Fig. 1) or the shell (Fig. 2), sharing common points of application and identical characteristics. The ensuing analysis aims to ascertain the SSS of the body.

To solve the problem, we will use coordinate systems moving together with the load: Cartesian $(x, y, \eta = z - ct)$ and cylindrical $(r, \theta, \eta = z - ct)$. In these coordinate systems, the motion of the body and the shell will be described by equations (1) and (2), respectively. [1, 2]:

$$\left(M_p^{-2} - M_s^{-2}\right)\text{grad div}\,\mathbf{u} + M_s^{-2}\nabla^2\mathbf{u} = \partial^2\mathbf{u}/\partial\eta^2\,, \tag{1}$$

where $M_p = c/c_p$, $M_s = c/c_s$ – Mach numbers; $c_s = \sqrt{\mu/\rho}$, $c_p = \sqrt{(\lambda + 2\mu)/\rho}$ – the speeds of propagation of compression-expansion and shear waves in the body, $\lambda = 2\mu\nu/(1-2\nu)$; ∇^2 – Laplace operator, **u** – the displacement vector of the elastic body.

$$\begin{aligned}
&\left[1 - \frac{(1-\nu_0)\rho_0 c^2}{2\mu_0}\right]\frac{\partial^2 u_{0\eta}}{\partial\eta^2} + \frac{1-\nu_0}{2R^2}\frac{\partial^2 u_{0\eta}}{\partial\theta^2} + \frac{1+\nu_0}{2R}\frac{\partial^2 u_{0\theta}}{\partial\eta\partial\theta} + \frac{\nu_0}{R}\frac{\partial u_{0r}}{\partial\eta} = -\frac{1-\nu_0}{2\mu_0 h_0}q_\eta,\\
&\frac{1+\nu_0}{2R}\frac{\partial^2 u_{0\eta}}{\partial\eta\partial\theta} + \frac{(1-\nu_0)}{2}\left(1 - \frac{\rho_0 c^2}{\mu_0}\right)\frac{\partial^2 u_{0\theta}}{\partial\eta^2} + \frac{1}{R^2}\frac{\partial^2 u_{0\theta}}{\partial\theta^2} + \frac{1}{R^2}\frac{\partial u_{0r}}{\partial\theta} = \frac{1-\nu_0}{2\mu_0 h_0}(P_\theta - q_\theta),\\
&\frac{\nu_0}{R}\frac{\partial u_{0\eta}}{\partial\eta} + \frac{1}{R^2}\frac{\partial u_{0\theta}}{\partial\theta} + \frac{h_0^2}{12}\nabla^2\nabla^2 u_{0r} + \frac{(1-\nu_0)\rho_0 c^2}{2\mu_0}\frac{\partial^2 u_{0r}}{\partial\eta^2} + \frac{u_{0r}}{R^2} = -\frac{1-\nu_0}{2\mu_0 h_0}(P_r - q_r),
\end{aligned} \tag{2}$$

where q_j and u_{0j} – the response of the body and the displacements of points on the mid-surface of the shell (when $r = R$ $q_j = \sigma_{rj}$, where σ_{rj} – the stresses in the points of the body), $j = \eta, \theta, r$; $P_\theta(\theta, \eta)$ and $P_r(\theta, \eta)$ – the intensity of the torsional and normal load.

Let's express the vector **u** based on the Lamé potentials φ_j (j = 1, 2, 3) [11]

$$\mathbf{u} = \text{grad}\,\varphi_1 + \text{rot}(\varphi_2\mathbf{e}_\eta) + \text{rot rot}(\varphi_3\mathbf{e}_\eta), \tag{3}$$

where $\mathbf{e}_\eta$ – the unit vector of the axis η.

Using (1) and (3) we obtain:

$$\nabla^2\varphi_j = M_j^2\,\partial^2\varphi_j/\partial\eta^2\,,\ j = 1, 2, 3\,. \tag{4}$$

Here $M_1 = M_p$, $M_2 = M_3 = M_s$.

Let's represent the components of the SSS of the body using Lamé potentials φ_j.

The components of vector **u** (3) in Cartesian (5) and cylindrical (6) moving coordinate systems:

$$\begin{aligned}
u_x &= \frac{\partial\varphi_1}{\partial x} + \frac{\partial\varphi_2}{\partial y} + \frac{\partial^2\varphi_3}{\partial x\partial\eta},\\
u_y &= \frac{\partial\varphi_1}{\partial y} - \frac{\partial\varphi_2}{\partial x} + \frac{\partial^2\varphi_3}{\partial y\partial\eta},\\
u_\eta &= \frac{\partial\varphi_1}{\partial\eta} + m_s^2\frac{\partial^2\varphi_3}{\partial\eta^2};
\end{aligned} \tag{5}$$

$$\begin{aligned}
u_r &= \frac{\partial\varphi_1}{\partial r} + \frac{1}{r}\frac{\partial\varphi_2}{\partial\theta} + \frac{\partial^2\varphi_3}{\partial\eta\partial r},\\
u_\theta &= \frac{1}{r}\frac{\partial\varphi_1}{\partial\theta} - \frac{\partial\varphi_2}{\partial r} + \frac{1}{r}\frac{\partial^2\varphi_3}{\partial\eta\partial\theta},\\
u_\eta &= \frac{\partial\varphi_1}{\partial\eta} + m_s^2\frac{\partial^2\varphi_3}{\partial\eta^2}.
\end{aligned} \tag{6}$$

By applying Hooke's law and considering equations (5) and (6), we can derive the formulas for the components of the stress tensor in both Cartesian (7) and cylindrical (8) coordinates

$$\sigma_{\eta\eta} = (2\mu + \lambda M_p^2)\frac{\partial^2\varphi_1}{\partial\eta^2} + 2\mu m_s^2\frac{\partial^3\varphi_3}{\partial\eta^3},$$

$$\sigma_{yy} = \lambda M_p^2\frac{\partial^2\varphi_1}{\partial\eta^2} + 2\mu\left(\frac{\partial^2\varphi_1}{\partial y^2} - \frac{\partial^2\varphi_2}{\partial x\partial y} + \frac{\partial^3\varphi_3}{\partial y^2\partial\eta}\right),$$

$$\sigma_{xx} = \lambda M_p^2\frac{\partial^2\varphi_1}{\partial\eta^2} + 2\mu\left(\frac{\partial^2\varphi_1}{\partial x^2} + \frac{\partial^2\varphi_2}{\partial x\partial y} + \frac{\partial^3\varphi_3}{\partial x^2\partial\eta}\right),$$

$$\sigma_{x\eta} = \mu\left(2\frac{\partial^2\varphi_1}{\partial\eta\partial x} + \frac{\partial^2\varphi_2}{\partial y\partial\eta} + (1+m_s^2)\frac{\partial^3\varphi_3}{\partial\eta^2\partial x}\right), \tag{7}$$

$$\sigma_{\eta y} = \mu\left(2\frac{\partial^2\varphi_1}{\partial y\partial\eta} - \frac{\partial^2\varphi_2}{\partial x\partial\eta} + (1+m_s^2)\frac{\partial^3\varphi_3}{\partial y\partial\eta^2}\right),$$

$$\sigma_{xy} = 2\mu\left(\frac{\partial^2\varphi_1}{\partial x\partial y} - \frac{\partial^2\varphi_2}{\partial x^2} - \frac{m_s^2}{2}\frac{\partial^2\varphi_2}{\partial\eta^2} + \frac{\partial^3\varphi_3}{\partial x\partial y\partial\eta}\right);$$

$$\sigma_{\eta\eta} = (2\mu + \lambda M_p^2)\frac{\partial^2\varphi_1}{\partial\eta^2} + 2\mu m_s^2\frac{\partial^3\varphi_3}{\partial\eta^3},$$

$$\sigma_{\theta\theta} = \lambda M_p^2\frac{\partial^2\varphi_1}{\partial\eta^2} + \frac{2\mu}{r}\left(\frac{1}{r}\frac{\partial^2\varphi_1}{\partial\theta^2} + \frac{\partial\varphi_1}{\partial r} + \frac{1}{r}\frac{\partial\varphi_2}{\partial\theta} - \frac{\partial^2\varphi_2}{\partial r\partial\theta} + \frac{1}{r}\frac{\partial^3\varphi_3}{\partial\theta^2\partial\eta} + \frac{\partial^2\varphi_3}{\partial r\partial\eta}\right),$$

$$\sigma_{rr} = \lambda M_p^2\frac{\partial^2\varphi_1}{\partial\eta^2} + 2\mu\left(\frac{\partial^2\varphi_1}{\partial r^2} + \frac{1}{r}\frac{\partial^2\varphi_2}{\partial\theta\partial r} - \frac{1}{r^2}\frac{\partial\varphi_2}{\partial\theta} + \frac{\partial^3\varphi_3}{\partial r^2\partial\eta}\right),$$

$$\sigma_{r\eta} = \mu\left(2\frac{\partial^2\varphi_1}{\partial\eta\partial r} + \frac{1}{r}\frac{\partial^2\varphi_2}{\partial\theta\partial\eta} + (1+m_s^2)\frac{\partial^3\varphi_3}{\partial\eta^2\partial r}\right), \tag{8}$$

$$\sigma_{\eta\theta} = \mu\left(\frac{2}{r}\frac{\partial^2\varphi_1}{\partial\theta\partial\eta} - \frac{\partial^2\varphi_2}{\partial r\partial\eta} + \frac{(1+m_s^2)}{r}\frac{\partial^3\varphi_3}{\partial\theta\partial\eta^2}\right),$$

$$\sigma_{r\theta} = 2\mu\left(\frac{1}{r}\frac{\partial^2\varphi_1}{\partial\theta\partial r} - \frac{1}{r^2}\frac{\partial\varphi_1}{\partial\theta} - \frac{\partial^2\varphi_2}{\partial r^2} - \frac{m_s^2}{2}\frac{\partial^2\varphi_2}{\partial\eta^2} + \frac{1}{r}\frac{\partial^3\varphi_3}{\partial r\partial\eta\partial\theta} - \frac{1}{r^2}\frac{\partial^2\varphi_3}{\partial\eta\partial\theta}\right).$$

Applying the Fourier transformation in η to equations (4), we obtain

$$\nabla_2^2\varphi_j^* - m_j^2\xi^2\varphi_j^* = 0, \quad j = 1, 2, 3, \tag{9}$$

where $\varphi_j^*(r,\theta,\xi) = \int_{-\infty}^{\infty}\varphi_j(r,\theta,\eta)e^{-i\xi\eta}d\eta$, $m_j^2 = 1 - M_j^2$, $m_1 \equiv m_p, m_2 = m_3 \equiv m_s$, ∇_2^2 – two-dimensional Laplace operator.

Applying the Fourier transform to (5) – (8) in η, we obtain expressions for the transformants of displacements u_l^* and stresses σ_{lm}^* in Cartesian ($l,m = x,y,\eta$) and cylindrical ($l,m = r,\theta,\eta$) coordinates, represented by φ_j^*.

Let's impose a constraint on the speed of load movement, assuming it is less than the shear wave velocity in the body, i.e. $c < c_s$. Then $M_s < 1$ ($m_s > 0$), and the solutions of equations (9) can be represented as follows

$$\varphi_j^* = \Phi_j^{(1)} + \Phi_j^{(2)}. \tag{10}$$

Here $\Phi_j^{(1)} = \sum_{n=-\infty}^{\infty} a_{nj}K_n(k_j r)e^{in\theta}$, $\Phi_j^{(2)} = \int_{-\infty}^{\infty} g_j(\xi,\zeta)\exp\left(iy\zeta + (x-h)\sqrt{\zeta^2 + k_j^2}\right)d\zeta$, $K_n(kr)$ – MacDonald functions, $k_j = m_j\xi$; a_{nj}, $g_j(\xi,\zeta)$ – unknown functions and coefficients to be determined, $j = 1, 2, 3$.

In the Cartesian coordinates, the expressions for the transformants of potentials (10) will take the form:

$$\varphi_j^* = \int_{-\infty}^{\infty}\left[\frac{e^{-xf_j}}{2f_j}\sum_{n=-\infty}^{\infty}a_{nj}\Phi_{nj} + g_j(\xi,\zeta)e^{(x-h)f_j}\right]e^{iy\zeta}d\zeta\,. \qquad (11)$$

Here $f_j = \sqrt{\zeta^2 + k_j^2}, \Phi_{nj} = \left(\frac{\zeta + f_j}{k_j}\right)^n$, $j = 1, 2, 3.$

Let's express the functions $g_j(\xi,\zeta)$ by the coefficients a_{nj} ($j = 1, 2, 3$). To accomplish this, we will consider (11) and utilize the boundary conditions when $x = h$:

$$\sigma_{xx}^* = \sigma_{xy}^* = \sigma_{x\eta}^* = 0\,.$$

Extracting coefficients of $e^{iy\zeta}$ and equating them to zero, we derive a system of three algebraic equations from which we can deduce

$$g_j(\xi,\zeta) = \frac{1}{\Delta_*}\sum_{l=1}^{3}\Delta_{jl}^* e^{-hf_l}\sum_{n=-\infty}^{\infty}a_{nl}\Phi_{nl}\,. \qquad (12)$$

Here $\Delta_* = \left(2\rho_*^2 - \beta^2\right)^2 - 4\rho_*^2\sqrt{\rho_*^2 - \alpha^2}\sqrt{\rho_*^2 - \beta^2}$,

$$\Delta_{11}^* = \frac{\Delta_*}{2\sqrt{\rho_*^2 - \alpha^2}} - \frac{\left(2\rho_*^2 - \beta^2\right)^2}{\sqrt{\rho_*^2 - \alpha^2}}, \Delta_{12}^* = -2\zeta\left(2\rho_*^2 - \beta^2\right), \Delta_{13}^* = 2\xi\left(2\rho_*^2 - \beta^2\right)\sqrt{\rho_*^2 - \beta^2},$$

$$\Delta_{21}^* = -\frac{M_s^2}{m_s^2}\Delta_{12}^*, \quad \Delta_{22}^* = -\frac{\Delta_{**}}{2\sqrt{\rho_*^2 - \beta^2}}, \quad \Delta_{23}^* = -4\xi\zeta\frac{M_s^2}{m_s^2}\sqrt{\rho_*^2 - \alpha^2}\sqrt{\rho_*^2 - \beta^2},$$

$$\Delta_{31}^* = -\frac{\Delta_{13}^*}{m_s^2\xi^2}, \quad \Delta_{32}^* = \frac{\Delta_{21}^*}{\beta^2}, \quad \Delta_{33}^* = -\frac{\Delta_{**}}{2\sqrt{\rho_*^2 - \beta^2}} + \frac{\left(2\rho_*^2 - \beta^2\right)^2}{\sqrt{\rho_*^2 - \beta^2}},$$

$$\alpha = M_p\xi, \quad \beta = M_s\xi, \quad \rho_*^2 = \xi^2 + \zeta^2, \quad \Delta_{**} = \left(2\rho_*^2 - \beta^2\right)^2 - 4\rho_{**}^2\sqrt{\rho_*^2 - \alpha^2}\sqrt{\rho_*^2 - \beta^2},$$

$$\rho_{**}^2 = \xi^2 + \left(2/m_s^2 - 1\right)\zeta^2.$$

As demonstrated in [1], the determinant $\Delta_*(\xi,\zeta) \neq 0$ for $c < c_R$, where c_R – the Rayleigh surface wave velocity in the half-space [11].

When $c < c_R$, the expressions (11), taking into account (12), will have the following form

$$\varphi_j^* = \int_{-\infty}^{\infty}\left[\frac{e^{-xf_j}}{2f_j}\sum_{n=-\infty}^{\infty}a_{nj}\Phi_{nj} + e^{(x-h)f_j}\sum_{l=1}^{3}\frac{\Delta_{jl}^*}{\Delta_*}e^{-hf_l}\sum_{n=-\infty}^{\infty}a_{nl}\Phi_{nl}\right]e^{iy\zeta}d\zeta\,. \qquad (13)$$

Substituting (13) into the expressions for u_l^* and σ_{lm}^* presented in the Cartesian ($l, m = x, y, \eta$) coordinates, we obtain:

$$u_l^* = \int_{-\infty}^{\infty}\sum_{j=1}^{3}\left(T_{lj}^{(1)}F_{nj}^{(1)} + T_{lj}^{(2)}F_{nj}^{(2)}\right)e^{i(y\zeta+\xi\eta)}d\zeta,$$

$$\frac{\sigma_{lm}^*}{\mu} = \int_{-\infty}^{\infty}\sum_{j=1}^{3}\left(S_{lmj}^{(1)}F_{nj}^{(1)} + S_{lmj}^{(2)}F_{nj}^{(2)}\right)e^{i(y\zeta+\xi\eta)}d\zeta\,.$$

Here:

$$F_{nj}^{(1)} = \frac{e^{-xf_j}}{2f_j}\sum_{n=-\infty}^{n=\infty}a_{nj}\Phi_{nj}, \quad F_{nj}^{(2)} = e^{(x-h)f_j}\sum_{k=1}^{3}\frac{\Delta_{jk}^*}{\Delta_*}e^{-hf_k}\sum_{n}a_{nk}\Phi_{nk}\,,$$

$$T_{x1}^{(1)} = -T_{x1}^{(2)} = -f_1, \quad T_{x2}^{(1)} = T_{x2}^{(2)} = -\zeta, \quad T_{x3}^{(1)} = -T_{x3}^{(2)} = f_3\xi\,,$$

$T_{y1}^{(1)} = T_{y1}^{(2)} = i\zeta, \quad T_{y2}^{(1)} = -T_{y2}^{(2)} = if_2, \quad T_{y3}^{(1)} = T_{y3}^{(2)} = -i\xi\zeta$,

$T_{\eta 1}^{(1)} = T_{\eta 1}^{(2)} = i\xi, \quad T_{\eta 2}^{(1)} = T_{\eta 2}^{(2)} = 0, \quad T_{\eta 3}^{(1)} = T_{\eta 3}^{(2)} = -im_s^2\xi^2$,

$S_{xx1}^{(1)} = S_{xx1}^{(2)} = n_2 + 2(f_1^2 - \xi^2 m_p^2), \quad S_{xx2}^{(1)} = -S_{xx2}^{(2)} = 2\zeta f_2, \quad S_{xx3}^{(1)} = S_{xx3}^{(2)} = -2f_3^2\xi$,

$S_{yy1}^{(1)} = S_{yy1}^{(2)} = n_2 - 2(\zeta^2 + \xi^2 m_p^2), \quad S_{yy2}^{(1)} = -S_{yy2}^{(2)} = -2f_2\zeta, \quad S_{yy3}^{(1)} = S_{yy3}^{(2)} = 2\xi\zeta^2$,

$S_{\eta\eta 1}^{(1)} = S_{\eta\eta 1}^{(2)} = n_2 - 2n_1, \quad S_{\eta\eta 2}^{(1)} = S_{\eta\eta 2}^{(2)} = 0, \quad S_{\eta\eta 3}^{(1)} = S_{\eta\eta 3}^{(2)} = 2m_s^2\xi^3$,

$S_{xy1}^{(1)} = -S_{xy1}^{(2)} = -2f_1\zeta i, \quad S_{xy2}^{(1)} = S_{xy2}^{(2)} = -(f_2^2 + \zeta^2)i, \quad S_{xy3}^{(1)} = -S_{xy3}^{(2)} = 2f_3\xi\zeta i$,

$S_{\eta y1}^{(1)} = S_{\eta y1}^{(2)} = -2\xi\zeta, \quad S_{\eta y2}^{(1)} = -S_{\eta y2}^{(2)} = -\xi f_2, \quad S_{\eta y3}^{(1)} = S_{\eta y3}^{(2)} = n_2\zeta$,

$S_{x\eta 1}^{(1)} = -S_{x\eta 1}^{(2)} = -2f_1\xi i, \quad S_{x\eta 2}^{(1)} = S_{x\eta 2}^{(2)} = -\xi\zeta i, \quad S_{x\eta 3}^{(1)} = -S_{x\eta 3}^{(2)} = n_2 f_3 i$,

$n_1 = (1 + m_p^2)\xi^2, \quad n_2 = (1 + m_s^2)\xi^2$.

To represent the transforms of potentials (7) in the cylindrical coordinate system, we will use the relationship [12]

$$\exp\left(iy\zeta + (x-h)\sqrt{\zeta^2 + k^2}\right) = \sum_{n=-\infty}^{\infty} I_n(kr)e^{in\theta}\left(\frac{\zeta + \sqrt{\zeta^2 + k^2}}{k}\right)^n e^{-h\sqrt{\zeta^2+k^2}}.$$

Here $I_n(kr)$ – modified Bessel functions.

Then

$$\varphi_j^* = \sum_{n=-\infty}^{\infty}\left(a_{nj}K_n(k_j r) + I_n(k_j r)\int_{-\infty}^{\infty} g_j(\xi,\zeta)\,\Phi_{nj}e^{-hf_j}d\zeta\right)e^{in\theta}.$$

When $c < c_R$, these expressions taking into account (12), will take the form

$$\varphi_j^* = \sum_{n=-\infty}^{\infty}\left(a_{nj}K_n(k_j r) + b_{nj}I_n(k_j r)\right)e^{in\theta}, \tag{14}$$

where $b_{nj} = \sum_{l=1}^{3}\sum_{m=-\infty}^{\infty} a_{ml}A_{nj}^{ml}$, $A_{\eta j}^{ml} = \int_{-\infty}^{\infty}\frac{\Delta_{jl}^*}{\Delta_*}\Phi_{ml}\Phi_{nj}e^{-h(f_l+f_j)}d\zeta$.

By substituting (14) into the expressions for u_l^* and σ_{lm}^* represented in the cylindrical ($l, m = r,\ \theta, \eta$) coordinate system, we obtain

$$u_l^* = \sum_{n=-\infty}^{\infty}\sum_{j=1}^{3}\left[T_{lj}^{(1)}\left(K_n(k_j r)\right)a_{nj} + T_{lj}^{(2)}\left(I_n(k_j r)\right)b_{nj}\right]e^{i(\xi\eta + n\theta)},$$

$$\frac{\sigma_{lm}^*}{\mu} = \sum_{n=-\infty}^{\infty}\sum_{j=1}^{3}\left[S_{lmj}^{(1)}\left(K_n(k_j r)\right)a_{nj} + S_{lmj}^{(2)}\left(I_n(k_j r)\right)b_{nj}\right]e^{i(\xi\eta + n\theta)}.$$

Here:

$T_{r1}^{(1)} = k_1 K_n'(k_1 r), \quad T_{r2}^{(1)} = -\frac{n}{r}K_n(k_2 r), \quad T_{r3}^{(1)} = -\xi k_3 K_n'(k_3 r)$,

$T_{\theta 1}^{(1)} = \frac{n}{r}K_n(k_1 r)i, \quad T_{\theta 2}^{(1)} = -k_2 K_n'(k_2 r)i, \quad T_{\theta 3}^{(1)} = -\frac{n}{r}\xi K_n(k_3 r)i$,

$T_{\eta 1}^{(1)} = \xi K_n(k_1 r)i, \quad T_{\eta 2}^{(1)} = 0, \quad T_{\eta 3}^{(1)} = -k_3^2 K_n(k_3 r)i$,

$S_{rr1}^{(1)} = 2\left(k_1^2 + \frac{n^2}{r^2} - \frac{\lambda M_p^2\xi^2}{2\mu}\right)K_n(k_1 r) - \frac{2k_1 K_n'(k_1 r)}{r}$, $S_{rr2}^{(1)} = \frac{2n}{r^2}K_n(k_2 r) - \frac{2k_2 K_n'(k_2 r)}{r}$,

$S_{rr3}^{(1)} = -2\xi\left(k_3^2 + \frac{n^2}{r^2}\right)K_n(k_3 r) + \frac{2\xi k_3 K_n'(k_3 r)}{r}$,

$S_{\theta\theta 1}^{(1)} = -2\left(\frac{n^2}{r^2} + \frac{\lambda M_p^2 \xi^2}{2\mu}\right) K_n(k_1 r) + \frac{2k_1 K_n'(k_1 r)}{r}$, $S_{\theta\theta 2}^{(1)} = -\frac{2nK_n(k_2 r)}{r^2} + \frac{2nk_2 K_n'(k_2 r)}{r}$,

$S_{\theta\theta 3}^{(1)} = \frac{2\xi n^2 K_n(k_3 r)}{r^2} - \frac{2\xi k_3 K_n'(k_3 r)}{r}$,

$S_{\eta\eta 1}^{(1)} = -2\xi^2\left(\frac{1+\lambda M_p^2}{2\mu}\right) K_n(k_1 r)$, $S_{\eta\eta 2}^{(1)} = 0$, $S_{\eta\eta 3}^{(1)} = 2m_3^2 \xi^3 K_n(k_3 r)$,

$S_{r\theta 1}^{(1)} = \left(-\frac{2nK_n(k_1 r)}{r^2} + \frac{2nk_1 K_n'(k_1 r)}{r}\right) i$, $S_{r\theta 2}^{(1)} = \left(-\left(k_2^2 + \frac{2n^2}{r^2}\right) K_n(k_2 r) + \frac{2k_2 K_n'(k_2 r)}{r}\right) i$,

$S_{r\theta 3}^{(1)} = \left(\frac{2n\xi K_n(k_3 r)}{r^2} - \frac{2n\xi k_3 K_n'(k_3 r)}{r}\right) i$,

$S_{\theta\eta 1}^{(1)} = -\frac{2n\xi K_n(k_1 r)}{r}$, $S_{\theta\eta 2}^{(1)} = \xi k_2 K_n'(k_2 r)$, $S_{\theta\eta 3}^{(1)} = \frac{n\xi^2(1+m_3^2) K_n(k_3 r)}{r}$,

$S_{r\eta 1}^{(1)} = 2\xi k_1 K_n'(k_1 r) i$, $S_{r\eta 2}^{(1)} = -\frac{\xi n K_n(k_2 r) i}{r}$, $S_{r\eta 3}^{(1)} = -\xi^2 k_3 (1+m_3^2) K_n'(k_3 r) i$;

$K_n'(kr) = \frac{dK_n(kr)}{d(kr)}$; $T_{lj}^{(2)}$, $S_{lmj}^{(2)}$ are obtained from $T_{lj}^{(1)}$, $S_{lmj}^{(1)}$ by replacing $K_n(k_j r)$ with $I_n(k_j r)$.

To determine the unknown coefficients a_{nj} (j = 1, 2, 3) in the expressions for the transformants of displacements u_l^* and stresses σ_{lm}^*, we will use the boundary conditions at $r = R$:

- for a nonreinforced cavity (Fig. 1)

$$\sigma_{rr}^* = P_r^*(\theta, \xi), \ \sigma_{r\theta}^* = -P_\theta^*(\theta, \xi), \ \sigma_{r\eta}^* = 0, \tag{15}$$

where $P_j^*(\theta, \xi) = \int_{-\infty}^{\infty} P_j(\theta, \eta) e^{-i\xi\eta} d\eta = p_j(\theta) p_j^*(\xi)$, $p_j(\theta) = \sum_{n=-\infty}^{\infty} P_{nj} e^{in\theta}$, $p_j^*(\xi) = \int_{-\infty}^{\infty} p_j(\eta) e^{-i\xi\eta} d\eta$, $j = r, \theta$;

- for cavity reinforcement with a thin shell (Fig. 2)

$$u_l^* = u_{0l}^*, \tag{16}$$

where $u_{0l}^*(\theta, \xi) = \int_{-\infty}^{\infty} u_{0l}(\theta, \eta) e^{-i\xi\eta} d\eta$, $l = \eta, \theta, r$.

By applying the Fourier transformation to (2) in η and expanding the functions $P_j^*(\theta, \xi)$ and $u_{0l}^*(\theta, \xi)$ ($j = \theta, r$, $l = \eta, \theta, r$) into Fourier series in η, we obtain:

$$\varepsilon_1^2 u_{0n\eta} + \nu_2 n\xi_0 u_{0n\theta} - 2i\nu_0 \xi_0 u_{0nr} = -G_0 q_{n\eta},$$
$$\nu_2 n\xi_0 u_{0n\eta} + \varepsilon_2^2 u_{0n\theta} - 2inu_{0nr} = G_0 (P_{n\theta} - q_{n\theta}),$$
$$2i\nu_0 \xi_0 u_{0n\eta} + 2inu_{0n\theta} + \varepsilon_3^2 u_{0nr} = G_0 (P_{nr} - q_{nr}),$$

where $\varepsilon_1^2 = \alpha_0^2 - \varepsilon_0^2$, $\varepsilon_2^2 = \beta_0^2 - \varepsilon_0^2$, $\varepsilon_3^2 = \gamma_0^2 - \varepsilon_0^2$, $\varepsilon_0^2 = \nu_1 \xi_0^2 M_{s0}^2$, $\xi_0 = \xi R$,

$\alpha_0^2 = 2\xi_0^2 + \nu_1 n^2$, $\xi_0 = \xi R$, $\beta_0^2 = \nu_1 \xi_0^2 + 2n^2$, $\gamma_0^2 = \chi^2 (\xi_0^2 + n^2)^2 + 2$,

$\nu_1 = 1 - \nu_0$, $\nu_2 = 1 + \nu_0$, $M_{s0} = \frac{c}{c_{s0}}$, $c_{s0} = \sqrt{\frac{\mu_0}{\rho_0}}$, $\chi^2 = \frac{h_0^2}{6R^2}$, $G_0 = -\frac{\nu_1 R^2}{\mu_0 h_0}$; P_{nj} and u_{0nl} – the coefficients of decomposition $P_j^*(\theta, \xi)$ and $u_{0l}^*(\theta, \xi)$ in the Fourier series by θ; $q_{nl} = (\sigma_{rl}^*)_n$. When $r = R$, $j = \theta, r$, $l = \eta, \theta, r$.

By solving the last equations with respect to u_{0nl} ($l = \eta, \theta, r$) we find:

$$u_{0n\eta} = G_0 \sum_{j=1}^{3} \frac{\delta_{\eta j}}{\delta_n} (P_{nj} - q_{nj}),$$

$$u_{0n\theta} = G_0 \sum_{j=1}^{3} \frac{\delta_{0j}}{\delta_n} \left(P_{nj} - q_{nj}\right),$$

$$u_{0nr} = G_0 \sum_{j=1}^{3} \frac{\delta_{rj}}{\delta_n} \left(P_{nj} - q_{nj}\right).$$

Here $\delta_n = (\varepsilon_1\varepsilon_2\varepsilon_3)^2 - (\varepsilon_1\xi_1)^2 - (\varepsilon_2\xi_2)^2 + 2\xi_1\xi_2\xi_3$, $\delta_{\eta 1} = (\varepsilon_2\varepsilon_3)^2 - \xi_1^2$, $\delta_{\eta 2} = D_1$, $\delta_{\eta 3} = iD_2$, $\delta_{\theta 1} = D_1$, $\delta_{\theta 2} = (\varepsilon_1\varepsilon_3)^2 - \xi_2^2$, $\delta_{\theta 3} = iD_3$, $\delta_{r1} = -iD_2$, $\delta_{r2} = -iD_3$, $\delta_{r3} = (\varepsilon_1\varepsilon_2)^2 - \xi_3^2$, $\xi_1 = 2n$, $\xi_2 = 2\nu_0\xi_0$, $\xi_3 = \nu_2\xi_0 n$, $D_1 = \xi_0 n\left(4\nu_0 - \varepsilon_3^2\nu_2\right)$, $D_2 = 2\xi_0\left(\varepsilon_2^2\nu_0 - n^2\nu_2\right)$, $D_3 = 2n\left(\varepsilon_1^2 - \xi_0^2\nu_0\nu_2\right)$; $P_{n1} = P_{m\eta} = 0$, $P_{n2} = P_{n\theta}$, $P_{n3} = P_{nr}$, $q_{n1} = q_{m\eta}$, $q_{n2} = q_{n\theta}$, $q_{n3} = q_{nr}$.

By substituting the respective expressions into the boundary conditions (15) or (16) and equating the coefficients of the series with respect to $e^{in\theta}$, for each value of $n = 0, \pm 1, \pm 2, \ldots$, we obtain a system of linear algebraic equations with the determinant $\Delta_n(\xi, c) \neq 0$, from which we find the coefficients a_{nj} (j = 1, 2, 3). Next, by applying the inverse Fourier transform, we compute the displacements u_l and stresses σ_{lm} (l, m = r, θ, η) in the body. In this case, any numerical method can be used, provided that the determinant $\Delta_n(\xi, c) \neq 0$ for each value of $n = 0, \pm 1, \pm 2, \ldots$. Research on determinants $\Delta_n(\xi, c)$ has demonstrated that for an unsupported cavity (Fig. 1), this requirement can be fulfilled by satisfying the condition $c < c_R$. However, for a supported cavity (Fig. 2), the speed of load movement must be lower than its critical speeds $c < c_{(n)^*}$. The values of the critical speeds $c_{(n)^*}$ are determined from the equations $\Delta_n(\xi, c) = 0$. As studies of these equations based on numerical calculations show, the smallest (lowest) critical speed of the load corresponds to the number n = 0 ($\min c_{(n)^*} = c_{(0)^*}$) [1].

Results and Discussion

As an example, let's consider the circular cylindrical cavity depicted in Figure 1 with a radius of R = 1m in a half-space (h = 2R) with the following physical and mechanical properties: $\nu = 0{,}2$, $\mu = 2{,}532 \cdot 10^9$ Pa, $\rho = 2{,}5 \cdot 10^3$ kg/m^3 ($c_s = 1006{,}4$ m/s, $c_R = 917$ m/s). Along its surface, in the direction of the z-axis, an axisymmetric compressive normal load P_r and an axisymmetric torsional load P_θ of equal intensity, P (Pa), are moving with a constant velocity of c = 100 m/s. The loads are uniformly distributed within the interval $|\eta| \le l_0 = 0{,}2R$. In this case, $P_{0j} = 1$, $P_{nj} = 0$ ($n = \pm 1, \pm 2, \ldots$, $j = \theta, r$), $p_r^*(\xi) = -2P\sin(\xi l_0)/\xi$, $p_\theta^*(\xi) = P\sin(\xi l_0)/\xi$. We select the intensities P of the loads in such a way that for each of them, the total load over the entire length of the loading section $2l_0$ equals the equivalent concentrated radial load with an intensity of $P^{\circ\circ}$ (N/m), i.e. $P = P^{\circ\circ}/2l_0$. Then $p_r^*(\xi) = -P^{\circ\circ}\sin(\xi l_0)/(\xi l_0)$, $p_\theta^*(\xi) = P^{\circ\circ}\sin(\xi l_0)/(\xi l_0)$.

In Figure 3, the vertical $u_x^\circ = u_x\mu/P^\circ$, m ($a$) and horizontal $u_y^\circ = u_y\mu/P^\circ$, m ($b$) (where $P^\circ = P^{\circ\circ}$/m, Pa) displacements of the points of the boundary of the half-space are shown in the xy coordinate plane. Curves 1 are plotted for the case of an unsupported cavity (Fig. 1), while curves 2 are for the case when this cavity is reinforced with a thin cast iron (h_0 = 0,05 m; ν_0 = 0,3, $\mu_0 = 5{,}77 \cdot 10^{10}$ Pa, $\rho_0 = 7{,}2 \cdot 10^3$kg/m^3) shell (Fig. 2).

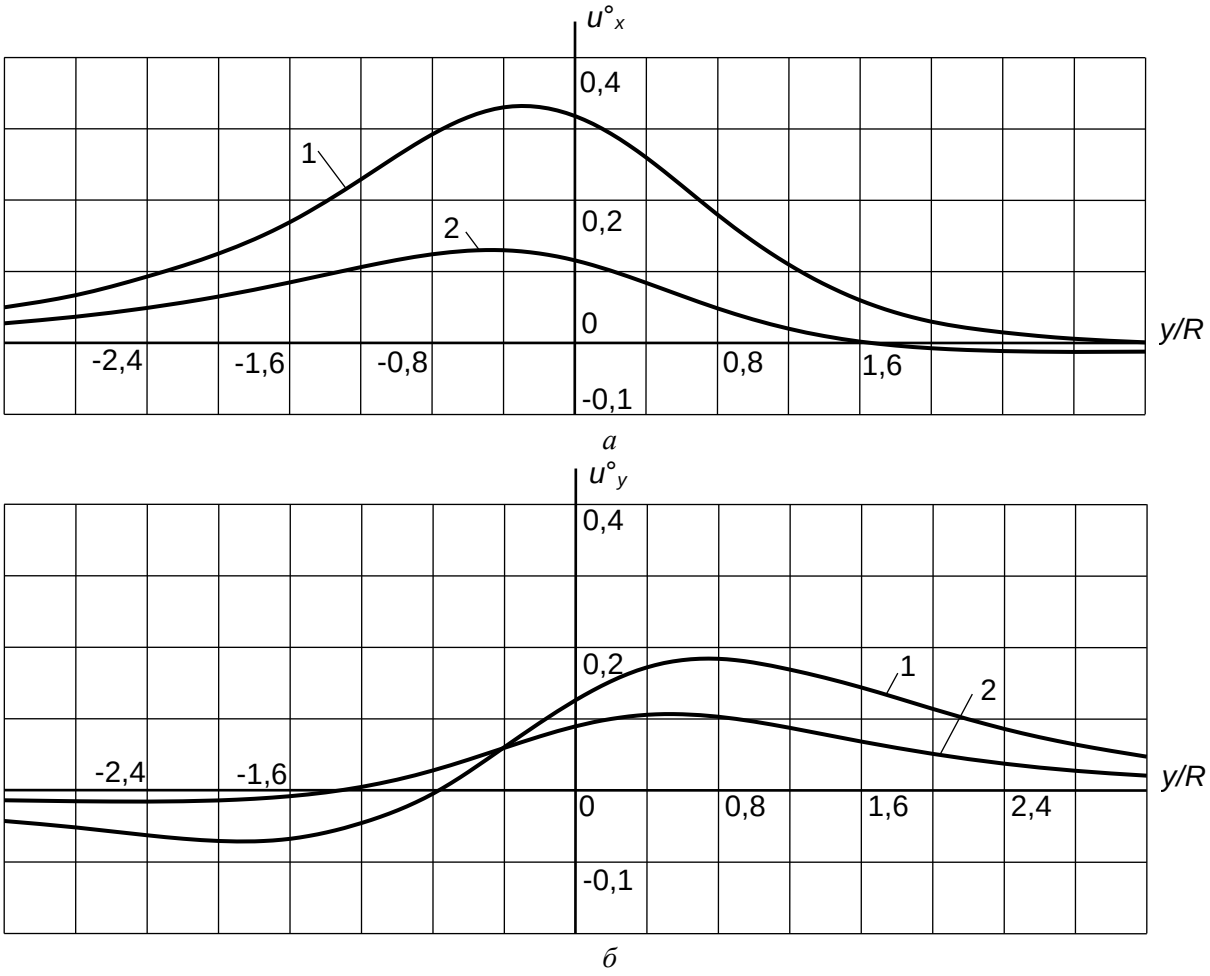

Figure 3. Displacements of points of the boundary of the half-space

From the analysis of the curves, it can be concluded that reinforcing the cavity with a shell leads to a reduction in the dynamic impact of moving loads on the boundary of the half-space.

Conclusion

The problem of the effect of uniformly moving normal and torsional loads along an elongated long circular cylindrical cavity, situated in an elastic half-space (body), on this elastic half-space has been solved. The cavity is either unreinforced or reinforced by a thin-walled elastic shell. Such loading action occurs during the rotational movement of cleaning devices in an underground pipeline and can also arise due to uneven dynamic loads transmitted to each of the rails laid in a cylindrical-shaped tunnel, whether it is supported with a shell or not. When solving the problem, the velocity of load movement is considered to be subsonic. Speed restrictions are imposed: in the case of an unsupported cavity, the speed must be lower than the Rayleigh wave velocity in the half-space, and in the case of a cavity supported by a shell, in addition, the speed must be lower than the critical speeds of the moving loads. In contrast to a similar problem for an elastic space that simulates a deep tunnel, this problem is more complicated, since it becomes necessary to take into account the waves reflected by the boundary of the half-space. In contrast to similar works where the medium is considered as an elastic space, this problem's solution takes into account the effect of waves reflected from the boundary of the half-space, which arise during the movement of loads.

Using the obtained solution and results of numerical experiments, the influence of the shell on the deformed state of the half-space boundary was studied under the action of uniformly applied axisymmetric normal and torsional loads moving at a constant speed within a certain range. The results of the study indicate that reinforcing the cavity with a shell leads to a reduction in the dynamic impact of moving loads on the boundary of the half-space.

References

1 Украинец В.Н. Динамика тоннелей и трубопроводов мелкого заложения под воздействием подвижных нагрузок / В.Н. Украинец. — Павлодар: Изд-во Павлодар. гос. ун-та, 2006. — 123 с.

2 Alexeyeva L.A. Dynamics of an elastic half-space with a reinforced cylindrical cavity under moving loads / L.A. Alexeyeva // International Applied Mechanics. — 2009. — Vol. 45, N 9. — P. 75-85. DOI: 10.1007/s10778-010-0238-z.

3 Coşkun İ. Dynamic Response of a Circular Tunnel in an Elastic Half Space / İ. Coşkun, D. Dolmaseven // Journal of Engineering. — 2017. — Vol. 2017. — 12 p. DOI: 10.1155/2017/6145375.

4 Yuan Z. Benchmark solution for vibrations from a moving point source in a tunnel embedded in a half-space / Z. Yuan, A. Boström, Y. Cai // Journal of Sound and Vibration. — 2017. — Vol. 387. — P. 177-193. DOI: 10.1016/j.jsv.2016.10.016.

5 Zhou Sh. Dynamics of Rail Transit Tunnel Systems / Shunhua Zhou. — Academic Press, 2019. — 276 p.

6 Coşkun İ. Dynamic stress and displacement in an elastic half-space with a cylindrical cavity / İ. Coşkun, H. Enginb, A. Özmutluc // Journal of Shock and Vibration. — 2011. — Vol. 18. — P. 827-838. DOI: 10.1155/2011/904936.

7 Пожуев В.И. Действие подвижной нагрузки на цилиндрическую оболочку в упругой среде / В.И. Пожуев // Строительная механика и расчет сооружений. — 1978. — № 1. — С. 44–48.

8 Пожуев В.И. Действие подвижной скручивающей нагрузки на цилиндрическую оболочку в упругой среде / В.И. Пожуев // Строительная механика и расчет сооружений. — 1984. — № 6. — С. 58–61.

9 Герштейн М.С. Задачи динамики магистральных трубопроводов / М.С. Герштейн, А.Т. Камерштейн, В.И. Прокофьев // Сб.: Расчёт пространственных конструкций. — Вып. 15. — М.: Стройиздат, 1973. — С. 78–86.

10 Дашевский М.А. Прогноз динамических воздействий на сооружения, расположенные вблизи трасс метро / М.А. Дашевский // Строит. механика и расчет сооружений. — 1982. — № 4. — С. 36–40.

11 Новацкий В. Теория упругости / В. Новацкий. — М.: Мир, 1975. — 872 с.

12 Ержанов Ж.С. Динамика тоннелей и подземных трубопроводов / Ж.С. Ержанов, Ш.М. Айталиев, Л.А. Алексеева. — Алма-Ата: Наука, 1989. — 240 с.

В.Н. Украинец, С.Р. Гирнис, К.Т. Макашев, В.Т. Станевич

Серпімді жартылай кеңістіктегі күшейтілмеген және күшейтілген қуысқа қозғалатын қалыпты және бұралу жүктемелерінің әрекеті

Серпімді жартылай кеңістікке (массивке) осы жартылай кеңістікте орналасқан шексіз ұзын дөңгелек цилиндрлік қуыстың жұқа қабырғасының серпімді қабығына бекітілмеген немесе бекітілген бойымен біркелкі қозғалатын қалыпты және бұралу жүктемелерінің әсері зерттелді. Жартылай кеңістік жүктердің әсерінен бос көлденең шекарасы қуыс осіне параллель болады. Жүктердің қозғалу жылдамдығы дыбысқа дейінгі деп қабылданады, яғни жартылай кеңістікте ығысу толқындарының таралу жылдамдығынан аз болады. Массив пен қабықтың қозғалысын сипаттау үшін сәйкесінше Ламе потенциалдарындағы серпімділік теориясының динамикалық теңдеулері және қабық теориясының классикалық теңдеулері пайдаланылған. Теңдеулер жүктемелермен бірге қозғалатын координаттар жүйелерінде (цилиндрлік немесе декарттық) ұсынылған. Жартылай кеңістіктің кернеулі–деформацияланған күйін (КДК) анықтау үшін интегралды Фурье түрлендіру әдісі қолданылады. Массив серпімді кеңістік түрінде ұсынылатын мұндай жұмыстардан айырмашылығы, мұнда есепті шешу кезінде жүктемелердің қозғалысы кезінде пайда болатын жартылай кеңістік шекарасымен шағылысқан толқындардың массивіне әсері ескеріледі. Есепті шешу және әзірленген компьютерлік бағдарламалар негізінде сандық эксперименттер жүргізілді. Сандық эксперименттердің нәтижелері белгілі бір аралықта біркелкі қолданылатын және қалыпты және бұралу жүктемелерінің осимметриялық тұрақты дыбысқа дейінгі және шектен кем қозғалатын жартылай кеңістік шекарасының деформацияланған күйіне қабықтың әсерін көрсететін графиктер түрінде берілген. Осы нәтижелерді талдаудан қуысты қабықпен нығайту қозғалмалы жүктемелердің жартылай кеңістік шекарасына динамикалық әсерінің төмендеуіне әкелетіні шығады.

Кілт сөздер: серпімді жартылай кеңістік, массив, қуыс, цилиндрлік қабық, қозғалмалы жүктеме, жылдамдық, қозғалыс, кернеу.

В.Н. Украинец, С.Р. Гирнис, К.Т. Макашев, В.Т. Станевич

Действие движущихся нормальной и скручивающей нагрузок на неподкреплённую и подкреплённую полость в упругом полупространстве

Исследовано воздействие на упругое полупространство (массив) нормальной и скручивающей нагрузок, равномерно движущихся вдоль неподкрепленной или подкреплённой тонкостенной упругой оболочкой бесконечно длинной круговой цилиндрической полости, находящейся в этом полупространстве. Свободная от действия нагрузок горизонтальная граница полупространства параллельна оси полости. Скорость движения нагрузок принимается дозвуковой, то есть меньше скорости распространения волн сдвига в полупространстве. Для описания движения массива и оболочки используются соответственно динамические уравнения теории упругости в потенциалах Ламе и уравнения классической теории оболочек. Уравнения представляются в перемещающихся вместе с нагрузками системах координат (цилиндрической или декартовой). Для определения напряженно-деформированного состояния полупространства используется метод интегрального преобразования Фурье. В отличие от подобных работ, где массив представляется в виде упругого пространства, здесь при решении задачи учитывается воздействие на массив отраженных границей полупространства волн, возникающих при движении нагрузок. На основе решения задачи и разработанных компьютерных программ проведены численные эксперименты. Результаты численных экспериментов представлены в виде графиков, которые иллюстрируют влияние оболочки на деформированное состояние границы полупространства при действии равномерно приложенных в определенном интервале и движущихся с постоянной дозвуковой и докритической скоростью осесимметричных нормальной и скручивающей нагрузок. Из анализа этих результатов следует, что подкрепление полости оболочкой приводит к снижению динамического воздействия движущихся нагрузок на границу полупространства.

Ключевые слова: упругое полупространство, массив, полость, цилиндрическая оболочка, подвижная нагрузка, скорость, перемещения, напряжения.

References

1 Ukrainets, V.N. (2006). Dinamika tonnelei i truboprovodov melkogo zalozheniia pod vozdeistviem podvizhnykh nagruzok [Dynamics of shallow tunnels and pipelines under the influence of moving loads]. Pavlodar: Izdatelstvo Pavlodarskogo gosudarstvennogo universiteta [in Russian].

2 Alexeyeva, L.A. (2009). Dynamics of an elastic half-space with a reinforced cylindrical cavity under moving loads. *International Applied Mechanics, Vol 45,* 9, 75-85.

3 Coşkun, İ., & Dolmaseven, D. (2017). Dynamic Response of a Circular Tunnel in an Elastic Half Space. *Journal of Engineering, Vol. 2017,* 12 p.

4 Yuan, Z., Boström, A., & Cai, Y. (2017). Benchmark solution for vibrations from a moving point source in a tunnel embedded in a half-space. *Journal of Sound and Vibration, Vol. 387,* 177-193.

5 Zhou, Sh. (2019). Dynamics of Rail Transit Tunnel Systems. Academic Press.

6 Coşkun, İ., Enginb H., & Özmutluc A. (2011). Dynamic stress and displacement in an elastic half-space with a cylindrical cavity. *Journal of Shock and Vibration, Vol. 18*, 827-838.

7 Pozhuev, V.I. (1978). Deistvie podvizhnoi nagruzki na tsilindricheskuiu obolochku v uprugoi srede [The action of a moving load on a cylindrical shell in an elastic medium]. *Stroitelnaia mekhanika i raschet sooruzhenii — Structural Mechanics and Structural Analysis*, 1, 44–48 [in Russian].

8 Pozhuev, V.I. (1984). Deistvie podvizhnoi skruchivaiushchei nagruzki na tsilindricheskuiu obolochku v uprugoi srede [The action of a moving torsional load on a cylindrical shell in an elastic medium]. *Stroitelnaia mekhanika i raschet sooruzhenii — Structural mechanics and calculation of structures*, 6, 58–61 [in Russian].

9 Gershtejn, M.S., Kamershtejn, A.T., & Prokof'ev, V.I. (1973). Zadachi dinamiki magistralnykh truboprovodov [Problems of the dynamics of main pipelines]. In *Raschet prostranstvennykh konstruktsii — Calculation of spatial structures*. Moscow: Stroiizdat, *15, 78–86* [in Russian].

10 Dashevskij, M.A. (1982). Prognoz dinamicheskikh vozdeistvii na sooruzheniia, raspolozhennye vblizi trass [Forecasting dynamic effects on structures located near subway lines]. *Stroitelnaia mekhanika i raschet sooruzhenii — Structural Mechanics and Structural Analysis*, 4, 36–40 [in Russian].

11 Novackij, V. (1975). Teoriia uprugosti [Theory of elasticity]. Moscow: Mir [in Russian].

12 Erzhanov, Zh.S., Ajtaliev, Sh.M., & Alekseeva, L.A. (1989). Dinamika tonnelei i podzemnykh truboprovodov [Dynamics of tunnels and underground pipelines]. Alma-Ata: Nauka [in Russian].